Power Flow Coloring System Over a Nanogrid With Fluctuating Power Sources and Loads

Saher Javaid, Takekazu Kato, *Member, IEEE*, and Takashi Matsuyama

***Abstract*—Due to the excessive increase in environmental costs of nonrenewable energy resources, there have been government legislation, policies, and new technologies to control carbon emissions. The increase in renewable resources requires new strategies for the operation and management of the electricity. This paper presents the power flow coloring system, which gives a unique ID to each power flow between a specific power source and a specific power load. It allows us to design multiple power flow patterns between distributed and fluctuating power sources and loads taking into account energy availability, cost, and carbon dioxide emission. For implementation, this paper proposes a cooperative distributed control method, where a master–slave role assignment scheme of power sources and a time-slot-based feedback control are introduced to cope with power fluctuations, while keeping the voltage stable. The experimental results clarify the practical feasibility of our proposed method in managing distributed fluctuating power sources and loads.**

***Index Terms*—Cooperative distributed control, energy on demand (EoD), i-Energy, nanogrid (NG), power flow coloring.**

I. Introduction

ACCORDING to the 21st session of conference of the parties, global warming is declared as one of the major global issues to be solved. Due to the excessive increase in environmental costs of nonrenewable resources, there have been regulations and international agreements to control CO_2 emissions [1]. To encourage rapid and sustained development of renewable energy sources, feed in tariff (FiT) is already commercially implemented by utilities in some countries. FiT systems typically oblige electric utilities to purchase renewable generated power at fixed price per kWh [2]. Moreover, the installation cost of renewable technologies is rapidly decreasing during recent years and slowly approaching grid parity (cost of generated power from alternative power source (PS), i.e., photovoltaic (PV), is equal to price of purchasing power from the grid) [3]. The expiration of FiT and decreasing costs for PV systems make an attractive choice for households and small communities to intentionally disconnect from the utility grid and start producing and consuming their own electricity [4].

Taking into account current market trends and future opportunities, major growth in small-scale power generation systems (PGSs) is observed. This is mainly because residential and commercial areas represent a major part of power consumption and carbon dioxide emissions and partly because small-scale PVs, wind turbines, fuel cells, and storage batteries have been introduced into houses, factories, and in offices. The large-scale penetration of small-scale PGSs results in drastic change in the structure of residential and commercial areas [5].

Nanogrid (NG) [6] is an example for such changing structures, which include multiple power generating sources, energy storage facilities, in-house power distribution system, and a variety of appliances. NGs have been studied significantly for future power distribution architecture from tens of kilowatts to megawatts leading to the microgrid (MG) level [7] and often operate over a simple shared power line. Moreover, an NG can be designed independently or can be associated with the national grid either for ac or dc power management [8]. As an NG is usually affiliated with the MG or the national grid, it has less problems as compared to the national wide grid in handling frequency stability, power loss, and reactive power.

In [9]–[11], the concept of the power flow coloring is proposed, which attaches the unique identification to each power flow between a pair of PS and power load (PL). Though the concept of the power flow coloring could be applied to any type of power grid, this paper particularly focuses on an NG. The reason is that the basic technologies can be developed for the implementation of the power flow coloring and facilitated in an NG consisting of a shared bus power line without complicated structures of power transmission and distribution.

The power flow coloring can manage multiple power flow streams with diverse characteristics. For example, unpredicted generated power by PVs can directly flow into a PL such as coolers/heaters without using storage buffers. The utilization of renewable sources can help in reducing the gas emissions. Moreover, the power flow coloring can assist in recognizing the cost-effective usage of power from different PSs. In our previous paper [11], the implementation of the power flow coloring over an NG was presented, which focused on fluctuating loads and

Manuscript received January 4, 2017; revised April 17, 2017, June 16, 2017, and July 18, 2017; accepted July 19, 2017. Date of publication August 2, 2017; date of current version December 1, 2017. This work was supported by JSPS Grants-in-Aid (KAKENHI) Grant JP16K12394 and i-Energy Joint Research Chair in Kyoto University. Paper no. TII-17-0020. *(Corresponding author: Saher Javaid.)*

S. Javaid and T. Matsuyama are with the Research Unit for Smart Energy Management, Center for the Promotion of Interdisciplinary Education and Research, Kyoto University, Kyoto 606-8501, Japan (e-mail: saherjavaid@i.kyoto-u.ac.jp; tm@i.kyoto-u.ac.jp).

T. Kato is with the Department of Electrical and Electronic Engineering, Faculty of Science and Technology, Shizuoka Institute of Science and Technology, Fukuroi 437-0032, Japan (e-mail: t.kato@ieee.org).

Color versions of one or more of the figures in this paper are available online at http://ieeexplore.ieee.org.

Digital Object Identifier 10.1109/TII.2017.2733550

fluctuating PS management is kept for future studies, while this paper gives a complete power flow coloring system over an NG with fluctuating PSs and PLs, while keeping the voltage stable.

The rest of this paper is organized as follows. Section II surveys related works and implementation methods of the power flow coloring. Section III shows representation and compilation of a power flow pattern (PFP) between multiple power devices. In Section IV, we propose an agent-based cooperative distributed system architecture. Section V introduces the system protocol with master–slave role assignment for PS agents and the time-slot-based feedback control (TSBFC) to cope with power fluctuations. In Section VI, the practicality of the power flow coloring system is demonstrated with experimental results. Section VII gives concluding remarks.

II. Related Works

The electricity market is experiencing significant changes because of large-scale integration of renewable energy resources from distribution level down to individual household.

The transactive energy (TE) [12] has received much attention and has been a part of many discussions these days. The TE is defined as a system of control and economic mechanisms that enables the dynamic balance of power supply and power demand across the entire electrical infrastructure. The growing penetration of rooftop PV systems bring both the variability of power supply and a need for utilities to coordinate the increasing number of variable loads to maintain a balanced and reliable system [13]. Our proposed power flow coloring system could be one of the possible solutions in near future.

Some readers might recognize similarities between the consignment power supply and the power flow coloring system, but both are different. First, the former handles volumes of power, and real-time power control is not required. The latter controls instantaneous power. Second, no explicit control is introduced for consignment supply because the amount of power is far less than the power managed; however, power flow coloring managed power over an NG of similar amount. That is, a sophisticated stability control mechanism should be developed. Third, the power flow coloring can manage dynamically fluctuating sources and loads, which is out of the scope of consignment power supply. In last, power flow coloring can manage power flows from multiple PSs to one load.

There are many implementation methods of the power flow coloring system classified as: power line switching, power routing, and synchronized source-load control. In [14], Okabe and Sakai proposed a matrix power line switch between a group of PSs and a group of loads. A physical power line connection is established between a PS and a load. While its control is simple, only one-to-one connection between a PS and a load can be realized and hard to scale up if the number of nodes grows. Takuno *et al.* [15] and Abe *et al.* [16] proposed power routing methods. They developed the so-called power routers that receive, store, and transmit chunks of power, power packets, just in the same way as message packet routers: a chunk of power is associated with source ID and destination ID. By introducing a multiplexing method, a simple power line can support multiple power packet transmissions. For realization, each router should be equipped with storage, which requires mass investments for the routing methods to be implemented in the existing grid.

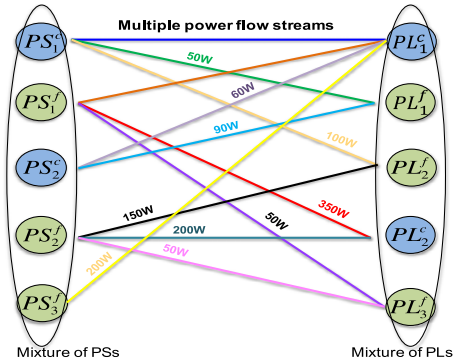

Fig. 1. Representation of a PFP.

The cooperative distributed control method for the power flow coloring system can be categorized as the synchronized source-load control method, which can be used inside a household and also for local community in an NG without much investments. Moreover, it manages power fluctuations of PSs and PLs by controlling terminal devices in real time, which is the technical advantage of our proposed method. For implementation, we introduce a cooperative distributed system consisting of power managers, PS agents, and load agents, which communicate with each other for the realization of the power flow coloring.

III. Representation and Compilation of a PFP

This section shows representation and compilation of a PFP between multiple PSs and PLs. A PS can supply electric power, e.g., solar panel, wind turbine, utility grid, etc., and a PL consumes electric power supplied by PS(s). Both power devices (PSs/ PLs) are classified into two categories, i.e., *controllable* and *fluctuating* based on their types, characteristics, and functionalities. A controllable PS/ PL can control its power (supply/consume) against power fluctuations, whereas fluctuating PS/ PL cannot control its power. All controllable and fluctuating power devices are considered with unique identifiers.

For example, all PSs (controllable and fluctuating) are indexed as PS_i^c $(i \in \{1, 2, \ldots, I\})$ and PS_j^f $(j \in \{1, 2, \ldots, J\})$, respectively, where I and J represent the total number of controllable PSs and fluctuating PSs. Similarly, all PLs comprising of controllable and fluctuating are represented with unique identifiers such as PL_k^c $(k \in \{1, 2, \ldots, K\})$ and PL_l^f $(l \in \{1, 2, \ldots, L\})$, where K and L show the total number of controllable PLs and fluctuating PLs. A power flow is defined as power flowing from a specific type of a PS to a specific type of PL(s). Each power flow is associated with some power levels in Watt. A PFP consists of multiple power flow streams between PSs and PLs, which can be represented by a colored bipartite graph (see Fig. 1). All power devices with both types are represented with different colors. It is also possible to represent a PFP with a matrix notation arranged in combination of multiple rows and columns. The rows and columns of the given matrix denote PSs and PLs (both types). Each element

of the given matrix is referred to a nominal power level in Watt supplied from a particular type of PS to specified PL. For example, P_{IK}^{cc} shows power flow from the Ith controllable PS to the Kth controllable PL, P_{IL}^{cf} denotes power flow from the Ith controllable PS to the Lth fluctuating PL, P_{JK}^{fc} represents power flow from the Jth fluctuating PS to the Kth controllable PL, and P_{JL}^{ff} shows power flow from the Jth fluctuating PS to the Lth fluctuating PL. Here, we assumed that given PFP satisfies all constraints on power supply and consumption, and a consistent and realizable PFP is designed by the system.

After matrix representation, compilation of PFP matrix starts. The compilation of a PFP is defined as a process that uses the given PFP matrix and measured power levels of fluctuating power devices to compute power levels for controllable power devices under the power balance constraint such that the total power supply from a PS is equal to the total power consumption of PLs attached with that particular PS.

$$\text{PFP} = \begin{array}{c} \\ \text{PS}_1^c \\ \text{PS}_2^c \\ \vdots \\ \text{PS}_I^c \\ \text{PS}_1^f \\ \text{PS}_2^f \\ \vdots \\ \text{PS}_J^f \end{array} \begin{array}{c} \begin{array}{cccc|cccc} \text{PL}_1^c & \text{PL}_2^c & \cdots & \text{PL}_K^c & \text{PL}_1^f & \text{PL}_2^f & \cdots & \text{PL}_L^f \end{array} \\ \left[\begin{array}{cccc|cccc} P_{11}^{cc} & P_{12}^{cc} & \cdots & P_{1K}^{cc} & P_{11}^{cf} & P_{12}^{cf} & \cdots & P_{1L}^{cf} \\ P_{21}^{cc} & P_{22}^{cc} & \cdots & P_{2K}^{cc} & P_{21}^{cf} & P_{22}^{cf} & \cdots & P_{2L}^{cf} \\ \vdots & \vdots & \ddots & \vdots & \vdots & \vdots & \ddots & \vdots \\ P_{I1}^{cc} & P_{I2}^{cc} & \cdots & P_{IK}^{cc} & P_{I1}^{cf} & P_{I2}^{cf} & \cdots & P_{IL}^{cf} \\ \hline P_{11}^{fc} & P_{12}^{fc} & \cdots & P_{1K}^{fc} & P_{11}^{ff} & P_{12}^{ff} & \cdots & P_{1L}^{ff} \\ P_{21}^{fc} & P_{22}^{fc} & \cdots & P_{2K}^{fc} & P_{21}^{ff} & P_{22}^{ff} & \cdots & P_{2L}^{ff} \\ \vdots & \vdots & \ddots & \vdots & \vdots & \vdots & \ddots & \vdots \\ P_{J1}^{fc} & P_{J2}^{fc} & \cdots & P_{JK}^{fc} & P_{J1}^{ff} & P_{J2}^{ff} & \cdots & P_{JL}^{ff} \end{array}\right] \end{array}.$$

Here, it is assumed that there are no communication and computation delays. As the physical power by a fluctuating power device varies a lot due to its nature and operation modes, the nominal power value specified in the PFP matrix is hard to maintain physically. Therefore, there is a need to design a compilation algorithm that can 1) link between physical power levels by power devices and nominal power levels in PFP matrix and 2) manage all possible power flow streams between PSs and PLs (with both types).

Our idea to devise the compilation algorithm is that the PFP matrix can be partitioned into the following four disjoint sectors, each of which can be processed independently of the others:

1) PFP between controllable PSs and controllable PLs;
2) PFP between controllable PSs and fluctuating PLs;
3) PFP between fluctuating PSs and controllable PLs;
4) PFP between fluctuating PSs and fluctuating PLs.

Here, "independent" refers to compilation of each sector that ensures its independent compilation process. Each sector has its own subalgorithm for compilation, which computes power levels for controllable power devices. This means the computation of power levels for controllable power devices in each sector is a partial computation of power for controllable power devices, and the overall power of a particular controllable power device can be achieved by summing up all partial computations during each sector's compilation process. Therefore, it is required to initialize the power levels of all controllable power devices (PSs/PLs) because, during the compilation process, controllable power devices will receive the target power level for power supply/consumption.

For example, the power supply of the ith controllable PS and power consumption by the kth controllable PL are initialized. The following initialization algorithm is required to initialize power levels of all attached controllable power devices. The compilation subalgorithms for each sector of the given PFP matrix are discussed in the following subsections.

Algorithm 1: Initialization of all controllable power PSs, (PS_i^c), and PLs, (PL_k^c).

```
for i = 1 to I do
  for k = 1 to K do
    W(PS_i^c) = W(PL_k^c) = 0
  end for
end for
```

A. PFP Between Controllable PSs and PLs

The compilation subalgorithm of the first sector of the PFP matrix is related to power flow streams between controllable PSs and controllable PLs only. Since all power devices are controllable, the power supply from PSs and power consumption by PLs can be controlled accurately according to the nominal power levels in Watt specified.

The given subalgorithm computes power levels for controllable power devices. For example, the specified power level in the PFP matrix, as P_{ik}^{cc}, is added to the total power supply of the ith controllable PS, $W(\text{PS}_i^c)$, and the total power consumption of the kth controllable PL, $W(\text{PL}_k^c)$.

Algorithm 2: For power flow streams between PS_i^c and PL_k^c.

```
for i = 1 to I do
  for k = 1 to K do
    W(PS_i^c) = P_ik^cc + W(PS_i^c)
    W(PL_k^c) = P_ik^cc + W(PL_k^c)
  end for
end for
```

B. PFP Between Controllable PSs and Fluctuating PLs

The subalgorithm of the second sector of the PFP matrix considers the power flow streams between controllable PSs and fluctuating PLs.

It is possible that fluctuating PL of this sector is further connected with fluctuating PS(s). In this case, the fluctuating PL with all power flow streams will be eliminated from the compilation process of the second sector (see Fig. 2). These eliminated power flow streams would be compiled together with sector 4 of the PFP matrix, which will be explained later. This means that

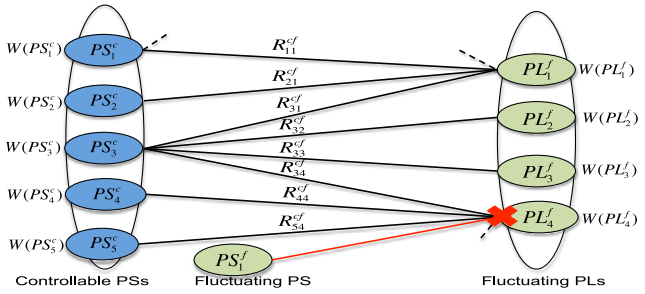

Fig. 2. Target power flow streams for compilation process of sector 2 of the PFP matrix.

the target power flow streams that can be handled with this subalgorithm consist of power flow streams between controllable PSs and fluctuating PLs only.

It is well known that the power consumption of fluctuating PLs fluctuates and sometimes varies a lot due to its operation modes (e.g., automatic power control in an air conditioner). This means that the nominal power value specified in the PFP matrix is just a reference and hard to maintain physically. To associate nominal power level given in the PFP matrix with physical power values of fluctuating PL, elements of sector 2 of the PFP matrix are converted to power ratios called *power supply ratio (PSR)*. The PSR can be computed as

$$\mathrm{PSR} = \left[R_{il}^{cf} \right] = \left[\frac{P_{il}^{cf}}{\sum_{i=1}^{I} P_{il}^{cf}} \right] \tag{1}$$

$$\sum_{i=1}^{I} R_{il}^{cf} = 1 \quad \text{for all } l$$

where P_{il}^{cf} and R_{il}^{cf} denote the nominal power level and the PSR supplied from the ith controllable PS to lth fluctuating.

The given subalgorithm for compilation of sector 2 of the PFP matrix computes power levels for controllable PSs, $W(\mathrm{PS}_i^c)$, when measured power consumption levels of fluctuating PLs, $W(\mathrm{PL}_l^f)$, and PFP are given. The ratio-based power levels of fluctuating PLs are added to the power supply of all controllable PSs, which supply power to those PLs. The target power flow streams are checked by $P_{jl}^{ff} = 0$, which shows no power flow streams between fluctuating power devices exist in this compilation process.

Algorithm 3: For power flow streams between PS_i^c and PL_l^f.

for $i = 1$ to I **do**
  for $l = 1$ to L such that for all $j = 1$ to J, $P_{jl}^{ff} = 0$ **do**
    $W(\mathrm{PS}_i^c) = R_{il}^{cf} \cdot W(\mathrm{PL}_l^f) + W(\mathrm{PS}_i^c)$
  end for
end for

C. PFP Between Fluctuating PSs and Controllable PLs

The compilation of the third sector of the PFP matrix is related to power flow streams between fluctuating PSs and controllable PLs. It is possible that the fluctuating PS of this sector is further attached with fluctuating PL(s). The same situation has already been discussed in the previous subsection that power flow streams between fluctuating power devices would be compiled together with the compilation process of sector 4. Thus, the target power flow streams that can be solved by the subalgorithm of this sector consists of fluctuating PSs and controllable PLs only. Due to the nature of fluctuating PSs e.g., PV, the generated power is not constant and stable. To deal with fluctuating generated power, the nominal power levels of sector 3 are converted to power ratios called *power consumption ratio (PCR)* for controllable PLs. The PCR can be computed as

$$\mathrm{PCR} = \left[R_{jk}^{fc} \right] = \left[\frac{P_{jk}^{fc}}{\sum_{k=1}^{K} P_{jk}^{fc}} \right] \tag{2}$$

$$\sum_{k=1}^{K} R_{jk}^{fc} = 1 \quad \text{for all } j$$

where P_{jk}^{fc} and R_{jk}^{fc} denote the nominal power level and the PCR consumed by the kth controllable PL supplied from the jth fluctuating PS. The power level for controllable PLs can be computed with the given subalgorithm when the PFP matrix and measured power supply levels of fluctuating PSs, $W(\mathrm{PS}_j^f)$, are given.

Algorithm 4: For power flow streams between PS_j^f and PL_k^c.

for $k = 1$ to K **do**
  for $j = 1$ to J such that for all $l = 1$ to L, $P_{jl}^{ff} = 0$ **do**
    $W(\mathrm{PL}_k^c) = R_{jk}^{fc} \cdot W(\mathrm{PS}_j^f) + W(\mathrm{PL}_k^c)$
  end for
end for

D. PFP Between Fluctuating PSs and PLs

The compilation of the last sector of the PFP matrix includes power flow streams between fluctuating devices and power flow streams eliminated from the compilation processes of sectors 2 and 3, respectively. Since the power flow streams consist of fluctuating power devices only, it is not possible to maintain the nominal power levels specified in the PFP matrix.

One idea to control flow of power between fluctuating power devices is to ask cooperation from controllable power devices. As these power flow streams cannot be controlled by fluctuating power devices alone, the support from controllable power devices can make it possible to control the power fluctuations of fluctuating power devices ($\mathrm{PS}^f/\mathrm{PL}^f$). This idea implies a constraint that each fluctuating power device of the power flow must be directly attached with at least one controllable power device; otherwise, it is not possible to control power supply or consumption of the fluctuating device.

For example, for a power flow from a fluctuating PS to a fluctuating PL, each fluctuating power device on both sides of the power flow must be directly attached with at least one controllable power device (see Fig. 3). Then, attached controllable power devices on both sides of the power flow can control the power fluctuations of fluctuating power devices. This means

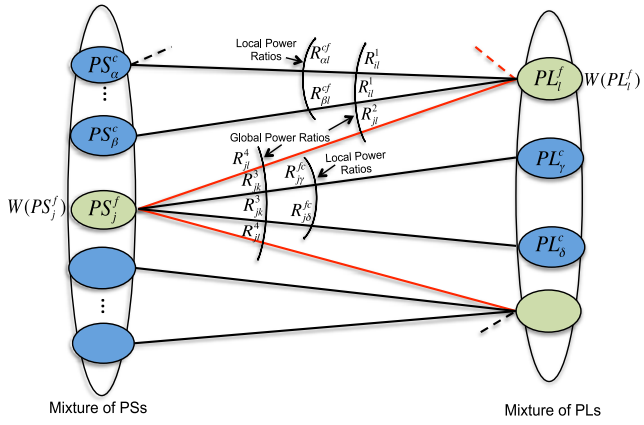

Fig. 3. PFP between fluctuating PSs and PLs.

compilation of this sector involves both types of power devices (i.e., controllable and fluctuating) on each side of a power flow. This makes the compilation of this sector "*Global*," that is, compilation of this sector should be done together with other sectors of the PFP matrix. For this reason, sectors 2 and 3 should be recompiled and ratio matrices need revision with global aspect. The recomputation of power ratios are named as *global power supply ratio (GPSR)* and *global power consumption ratio (GPCR)*.

Since computation of the GPSR considers both types of PSs with fluctuating PLs, i.e., sectors 2 and 4, while neglecting sector 3. The computation consists of two ratios: the first ratio, R^1_{il}, is used for sector 2, and the second ratio, R^2_{jl}, is applied on sector 4 of the PFP matrix

$$\text{GPSR} = \begin{bmatrix} R^1_{il} \\ R^2_{jl} \end{bmatrix} \tag{3}$$

$$R^1_{il} = \left[\frac{P^{cf}_{il}}{\sum_{i=1}^{I} P^{cf}_{il} + \sum_{j=1}^{J} P^{ff}_{jl}} \right] \tag{3a}$$

where P^{cf}_{il} denotes the nominal power level and R^1_{il} shows the ratio computation of sector 2 with global aspect

$$R^2_{jl} = \left[\frac{P^{ff}_{jl}}{\sum_{i=1}^{I} P^{cf}_{il} + \sum_{j=1}^{J} P^{ff}_{jl}} \right] \tag{3b}$$

where P^{ff}_{jl} represents the nominal power level and R^2_{jl} shows the ratio computation of sector 4 with global aspect. Similarly, the recomputation of the GPCR includes compilation of sectors 3 and 4 and neglects sector 2. The computation consists of two ratios: the first ratio, R^3_{jk}, is used for sector 3, and the second ratio, R^4_{jl}, is applied on sector 4

$$\text{GPCR} = \begin{bmatrix} R^3_{jk} & R^4_{jl} \end{bmatrix} \tag{4}$$

$$R^3_{jk} = \left[\frac{P^{fc}_{jk}}{\sum_{k=1}^{K} P^{fc}_{kl} + \sum_{l=1}^{L} P^{ff}_{jl}} \right] \tag{4a}$$

where P^{fc}_{jk} shows the nominal power level and R^3_{jk} is a computation of power ratio globally (with both types of PLs)

$$R^4_{jl} = \left[\frac{P^{ff}_{jl}}{\sum_{k=1}^{K} P^{fc}_{kl} + \sum_{l=1}^{L} P^{ff}_{jl}} \right] \tag{4b}$$

Algorithm 5: For power flow between PS^f_j and PL^f_l.

for $k = 1$ to K **do**
  for $j = 1$ to J such that $\exists\, l,\ P^{ff}_{jl} \neq 0$ **do**
    $W(\text{PL}^c_k) = R^3_{jk} \cdot W(\text{PS}^f_j) + W(\text{PL}^c_k)$
  end for
end for
for $i = 1$ to I **do**
  for $l = 1$ to L such that $\exists\, j,\ P^{ff}_{jl} \neq 0$) **do**
    $W(\text{PS}^c_i) = R^1_{il} \cdot W(\text{PL}^f_l) + W(\text{PS}^c_i)$
  end for
end for
for $j = 1$ to J **do**
  for $l = 1$ to L such that $P^{ff}_{jl} \neq 0$ **do**
    if $R^4_{jl} \cdot W(\text{PS}^f_j) \neq R^2_{jl} \cdot W(\text{PL}^f_l)$ **then**
      $W_{\min} = \text{Min}\left(R^4_{jl} \cdot W(\text{PS}^f_j), R^2_{jl} \cdot W(\text{PL}^f_l)\right)$
      $W^{\text{diff}}_j = R^4_{jl} \cdot W(\text{PS}^f_j) - W_{\min}$
      $W^{\text{diff}}_l = R^2_{jl} \cdot W(\text{PL}^f_l) - W_{\min}$
      if $W^{\text{diff}}_j > W^{\text{diff}}_l$ **then**
        for $k = 1$ to K **do**
          $W(\text{PL}^c_k) = R^{fc}_{jk} \cdot W^{\text{diff}}_j + W(\text{PL}^c_k)$
        end for
      else
        for $i = 1$ to I **do**
          $W(\text{PS}^c_i) = R^{cf}_{il} \cdot W^{\text{diff}}_l + W(\text{PS}^c_i)$
        end for
      end if
    end if
  end for
end for

where P^{ff}_{jl} denotes the nominal power level and R^4_{jl} is the power ratio computation with global aspect.

After the computation of global power ratios, the resultant matrix is used for power control Algorithm 5. The compiled resultant matrix is called *power flow specification (PFS)*; the size of this matrix is same as the original PFP matrix with four sectors. The first sector of the PFS matrix is same as the first sector of the PFP matrix, while sectors 2 and 3 are recomputed with global ratios as R^1_{il} and R^3_{jk}. Sector 4 uses two power ratios for each element as R^2_{jl} and R^4_{jl}.

The target power flow streams, power ratio computation, and ratio application can be explained with the help of Fig. 3, which shows two power flow streams between fluctuating power devices. Let PS^f_j be fluctuating PS, which supplies power to two fluctuating PLs. According to the constraint that each fluctuating power device on both sides of the power flow must be directly attached with at least one controllable power device, the controllable power devices are attached as PS^c_α, PS^c_β, PL^c_γ, PL^c_δ, and so on. The power level is assigned to each power device based on global ratio computations. Each power flow between fluctuating power devices has two global power ratios (e.g., R^2_{jl} and R^4_{jl} in Fig. 3), which introduces a conflict of power levels for the given

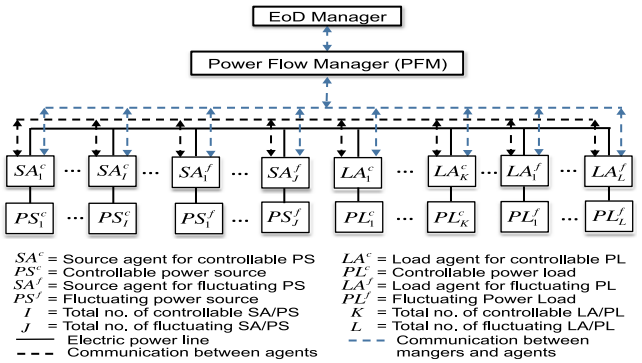

Fig. 4. System architecture.

power flow. In order to solve this conflict of power levels caused by two power ratios for the same power flow, the difference of power supply and consumption is computed by taking the minimum power level. The attached controllable power device with higher power difference compensates for power imbalance according to local power ratios (i.e., PSR/PCR calculated during compilation of sectors 2 and 3). For each power flow between fluctuating devices, Algorithm 5 is used to compute power levels for controllable devices when the PFP and measured power levels of fluctuating devices, $W(\mathrm{PS}_j^f)$ and $W(\mathrm{PL}_l^f)$, are given.

In the case of multiple power flow streams between fluctuating power devices, the system solves conflict one after the other. Additionally, if a fluctuating power device has multiple connections with other devices on the other side of the power flow, the assignment of power levels for fluctuating power devices is assigned prior than controllable power devices. The remaining power would be assigned to controllable power devices. Note that this is conflict resolution for the static system. For practical situations, we need a dynamic system protocol that can realize this static algorithm for power flow coloring.

IV. System Architecture

This section presents system architecture for implementation of the power flow coloring system over an NG (see Fig. 4). The proposed system is applicable to an NG (e.g., in a house, building, or local community), which consists of power managers, power agents, and multiple PSs and PLs with both types, i.e., controllable and fluctuating. All PSs and PLs are connected with a common electric power line. A power agent is attached to each PS/PL, which measures and controls power levels of the attached power device. The power agents attached with controllable power devices (PSs/PLs) are called controllable source agent (SA^c)/ load agent (LA^c). Similarly, the power agents associated with fluctuating devices (PSs/PLs) are named as fluctuating source agent (SA^f)/ load agent (LA^f).

All power agents cooperate with each other for the realization of the power flow coloring system. The proposed system is a distributed system, which manages two types of communication: 1) between managers and power agents, and 2) between all power agents. To maintain, specify, and monitor the overall PFP, two types of power managers are introduced: energy on demand (EoD) manager and power flow manager (PFM). The EoD manager is responsible for maintaining power profiles of PS/PL and conducting overall power management. Each profile contains characteristics of power device, i.e., minimum and maximum limitation of power levels, maximum number of power flows that a power device can handle, and availability of a power device at a particular time. The EoD manager receives *power demand requests (PDRs)* from all PLs. Based on the received PDRs, it mediates all power demands based on the EoD protocol and designs a consistent PFP specifying which PS should supply how many Watts to which PL. For the EoD protocol, see [18] and [19]. Then, the PFP is forwarded to the PFM, which monitors and coordinates all power agents to maintain the specified PFP. To bridge between nominal and physical power levels, the PFM compiles the given PFP matrix and computes the PFS matrix, which then broadcasts to all power agents so that the power ratios are preserved and the power flow coloring system realized.

V. System Protocol

This section describes the system protocol for the implementation of the power flow coloring system in practical situations. In a real-world scenario, it is required to manage power fluctuations by fluctuating PSs and PLs. Here, power fluctuations include three types of fluctuations: noisy fluctuations, power variations, and power mode changes. Noisy fluctuations are physical power fluctuations due to the nature of the fluctuating PSs and PLs. The power variations occur due to the internal feedback control of the power devices and change in power levels due to low power to/from high power. The power mode changes observe due to the transient behavior of power devices (e.g., ON/OFF status change) or triggered by the EoD manager, etc.

For implementation of power fluctuation management, a TSBFC method is introduced. The TSBFC method preserves the PFS designed by the PFM. That is, the TSBFC method can keep power ratios even if power fluctuations are caused by transient behaviors, nature of power devices, or mode change operations. The management of power fluctuations leads us to other problems to be solved. That is, a stability controller is required to maintain voltage stability of the NG against physical power fluctuations. For this purpose, the master and slave role assignment scheme is introduced among controllable SAs. Another expansion is required to cope with the real-world scenario because electric devices operate continuously without any break. As will be described later, the TSBFC method can be designed in a way to hide communication and computation delays. Finally, the proposed system protocol can satisfy above requirements for the implementation of the power flow coloring system with fluctuating PSs and PLs in real world.

A. Stability Controller

The power fluctuations caused by PSs and PLs can make the NG unstable leading to power blackout. To maintain voltage stability of the NG against power fluctuations, one of the controllable SAs is selected as master that works as voltage and phase sources. The master SA supplies and absorbs active

power (fluctuation) to keep the voltage level of the NG. The internal power control device and its corresponding controllable PS should be equipped with enough physical functions and power supply capacity to fulfill the role of the master PS, e.g., utility power line and a large storage battery. Note that, while the current implementation is designed for an ac power, it manages the active power alone and is to be revised to manage the reactive power.

All other controllable source agents operate as slaves. They work as active PSs/PLs and supply/consume specified powers. How to compute and modify the power specification for each slave SA^c/LA^c based on the given PFS, which will be described later. As for the physical implementation of master and slave, refer to Section V. Note that the master SA does not take care about specified supplying power. Additionally, when the entire power system includes multiple PSs that are capable to work as a master SA, the role of master can be switched dynamically based on the power system management policy, reserved for future study.

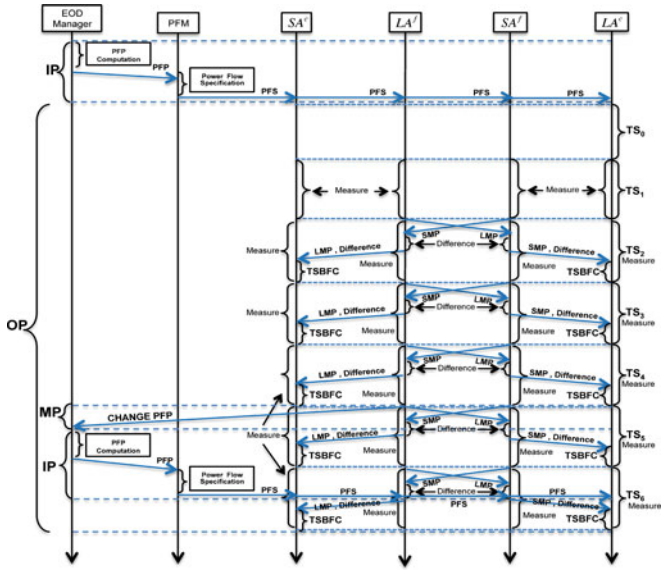

Fig. 5. System protocol.

B. TSBFC Method

The proposed method is developed to solve remaining problems: cope with unexpected power fluctuations of PSs and PLs while keeping the PFS. Also, the overlay execution of time slots (TSs) makes the power system work continuously without being effected by communication and computation delays. Hence, TSBFC is developed to solve these problems in a systematic way. Note that the proposed TSBFC is conducted by all slave power agents, and no explicit power control to comply with the PFS is conducted by the master SA.

1) TS and Protocol Description: The protocol consists of three phases: initialization phase (IP), operation phase (OP), and modification phase (MP). The EoD manager starts the IP by computing the PFP and send it to the PFM. Then, the PFM computes the PFS and broadcasts it to all power agents. This message is used for the synchronization between all power agents. After that, the OP starts by all power agents to implement assigned PFSs. The MP will start when any power agent observes an event that requires a change in the PFS. The event could be any change in user's behaviors and change in power consumption or supply. After observing such events, the power agent sends a CHANGE PFS message to the EoD manager, which then designs a new PFP to cope with the reported event and forwards it to the PFM. Finally, a new OP is started by the PFM. Note that the first OP will start after the IP; other OPs will execute in parallel with IPs and MPs because power devices supply/consume power continuously without any break.

At first, the time axis is divided into fixed length TSs. In Fig. 5, the OP is represented by a series of $TS_t (t = 0, 1, 2, \ldots)$. The first TS of the OP is TS_0; during this TS, the first sector of the PFS matrix is solved. That is, all power flow streams between controllable devices are fixed. In order to reduce the risks of sharp power peaks by turning ON devices, all controllable power devices start supplying or consuming power in pair one after other. In this TS, all controllable PSs and PLs reached some power level. In TS_1, all power agents with both types just measure power supply and consumption by their corresponding power devices.

During TS_2, each power agent associated with fluctuating power device sends its measured power (supply/consumption) to attached controllable power device(s). That is, all power flow streams between controllable and fluctuating power devices would be solved in this TS. In the case of power flow streams between fluctuating power devices, both fluctuating power devices exchange their measured power levels with each other. This exchange of power levels is done by message transmission. The message transmission from fluctuating SA is shown by *source measured power* while from fluctuating LA is shown as *load measured power* in Fig. 5. Upon receiving the measured information of previous TS (i.e., TS_1), each controllable agent computes the power level for the attached controllable power device to supply/consume in the next TS (i.e., TS_3). For power flow streams between fluctuating power devices, each fluctuating power agent saves this information to monitor the behavior of the other fluctuating device and also computes the difference between the received and its own measured power levels by taking the minimum power level. Then, the fluctuating power device with higher difference sends this power difference to the attached controllable power agent(s). The attached controllable power agent(s) compensates for the power imbalance by computing a new power level. Meanwhile, the power measurement is continued in TS_2 in parallel with communication and computation of power levels. Note that no power control is conducted for TS_0, TS_1, and TS_2.

In TS_t, $t \geq 3$, message exchange and computation of power levels for controllable power devices are conducted, while the power measurement also continued. Note that power control would be done in TS_3 for the measured power data of TS_1.

2) Feedback Control Method: The feedback control method is used by each slave agent to compute the target power for TS_t $t \geq 3$, which implements power control to maintain the specified PFS against unexpected power fluctuations of PSs and PLs.

Note that the algorithm processes average power consumption and supply levels in TS_t instead of instantaneous power levels. Let $W(\mathrm{SA}_i^c, t)$ and $W(\mathrm{SA}_j^f, t)$ be the average measured power levels by controllable and fluctuating SAs in TS_t. Similarly, $W(\mathrm{LA}_k^c, t)$ and $W(\mathrm{LA}_l^f, t)$ are the average measured power levels by controllable and fluctuating LAs in TS_t.

The implementation of feedback control considers remaining sectors of the PFS matrix, which includes fluctuating power devices, i.e., sectors 2, 3, and 4. To solve sectors 2 and 3, controllable power devices compute power levels by adding ratio-based power of the associated fluctuating power devices with Algorithms 3 and 4. Here, it is assumed that there are no control errors for controllable power devices to supply or consume computed power levels accurately.

For power flow streams between fluctuating devices, there is a need to evaluate the difference between the actual and measured power levels in TS_{t-2} by taking the minimum power level, $W(\min, t-2)$. Both fluctuating devices compute power difference, which is denoted as $W(\mathrm{SA}_j^{\mathrm{diff}}, t)$ and $W(\mathrm{SA}_l^{\mathrm{diff}}, t)$, which shows power difference computed by the jth fluctuating SA and the lth fluctuating LA in TS_t. The computations are given as

$$W(\mathrm{SA}_j^{\mathrm{diff}}, t) = \sum_{j=1}^{J} R_{jl}^4 \cdot W(\mathrm{SA}_j^f, t-2) + W(\mathrm{SA}_j^{\mathrm{diff}}, t-2) - W(\min, t-2) \quad (5)$$

$$W(\mathrm{LA}_l^{\mathrm{diff}}, t) = \sum_{l=1}^{L} R_{jl}^2 \cdot W(\mathrm{LA}_l^f, t-2) + W(LA_l^{\mathrm{diff}}, t-2) - W(\min, t-2) \quad (6)$$

where R_{jl}^4 and R_{jl}^2 are the GPSR and the GPCR, respectively. Based on the higher difference, the attached controllable device will compensate for the power imbalance, which is implemented in the next TS. The calculations of the power level are given as

$$W(\mathrm{SA}_i^c, t) = \sum_{l=1}^{L} R_{il}^{cf} \cdot W(\mathrm{LA}_l^{\mathrm{diff}}, t-2) + \sum_{l=1}^{L} R_{il}^{cf} \times W(\mathrm{LA}_l^f, t-2) + W(\mathrm{SA}_i^c, t-2) \quad (7)$$

$$W(\mathrm{LA}_k^c, t) = \sum_{j=1}^{J} R_{jk}^{fc} \cdot W(\mathrm{SA}_j^f, t-2) + \sum_{l=1}^{L} R_{jk}^{fc} \times W(\mathrm{SA}_l^f, t-2) + W(\mathrm{LA}_k^c, t-2). \quad (8)$$

Note that computation of power levels for controllable devices is done based on the local power ratio (i.e., R_{il}^{cf} and R_{jk}^{fc}). As noted before, when the PFS is modified, then a new OP will start from TS_t; some inter OP compensation processes should conducted, which is reserved for future study. When the EoD manager wants to change the PFS, it has to evaluate gaps between nominal and physical power based on the previous PFS and conduct some compensation processes before designing a new PFS.

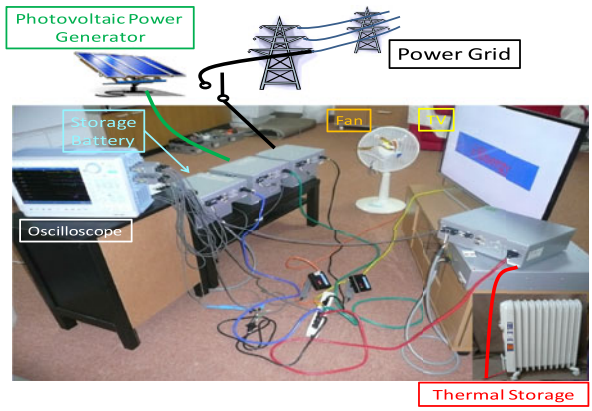

Fig. 6. Physical experiment setup.

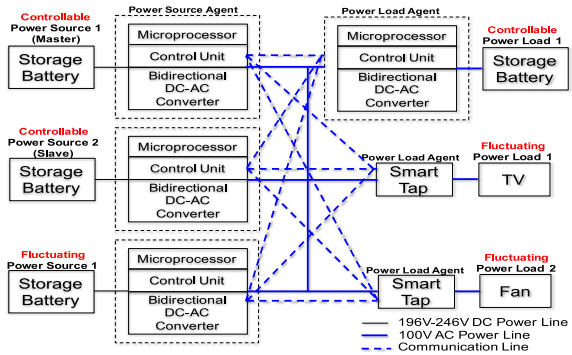

Fig. 7. Experiment setup.

VI. Experimental Results

The simulation results presented in this section verify that the proposed system works in real physical environments by managing all possible power flow streams, preserving local power ratios against power fluctuations, accommodating communication and computation delays, and maintaining voltage stability of the entire system. For implementation, hardware devices are developed for power sensing and control, i.e., power distributer and smart tap. A power distributer consists of a microprocessor, a bidirectional ac–dc converter, and a Zigbee wireless communication device. For technical details, refer to [20]. The real-time (i.e., 16.3-ms control interval) pulse width modulation control is conducted to make it work both as a voltage source (master PS) and as a PS (slave PS). Smart taps are power sensors with embedded microprocessors and ZigBee wireless communication devices [10].

The detailed power fluctuations of PSs and PLs are measured by an oscilloscope. All power agents associated with controllable PSs except master work as slaves. The phase and frequency control can be done both in a grid-connected or a grid-off mode. Figs. 6 and 7 illustrate physical and experimental settings for grid-off mode operation of our system.

In this experiment, four dc storage batteries via a power distributer, a TV, and a fan via smart taps are connected to a common ac 100-V power line. One of the storage batteries is selected as master (i.e., PS_1^c), second emulates as a PV PS (i.e., PS_1^f), which supplies fluctuating, third is used as slave (i.e., PS_2^c),

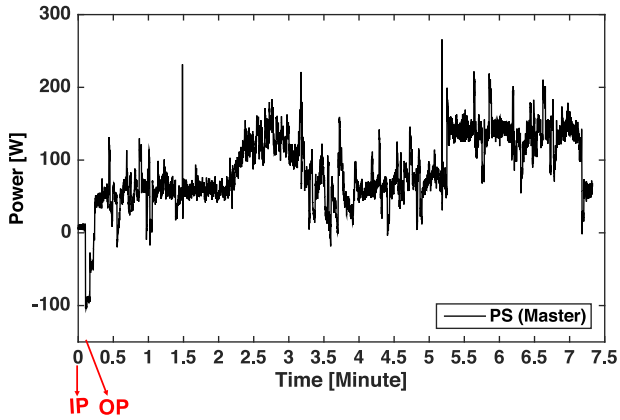

Fig. 8. Power supply of master PS.

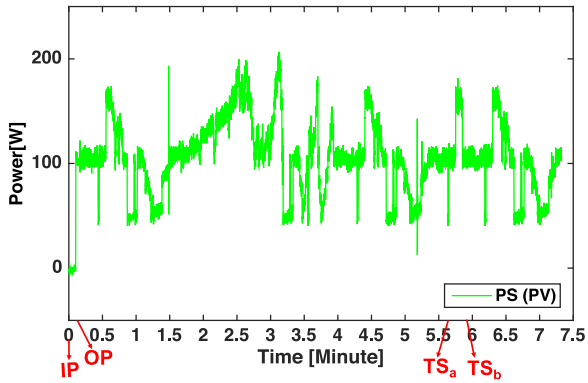

Fig. 9. Power supply of PV source.

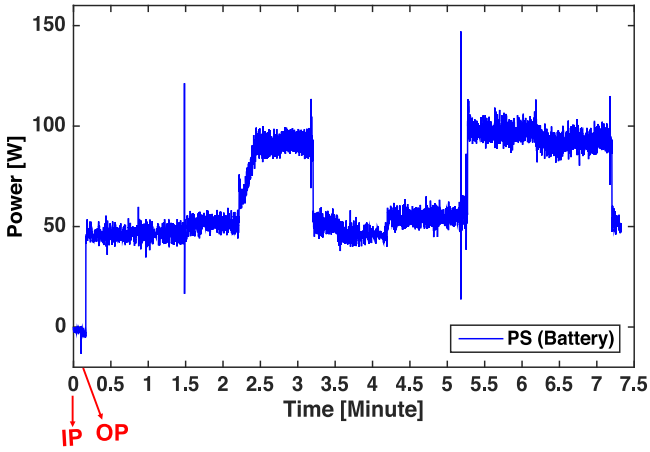

Fig. 10. Power supply of battery PS.

and remaining one is use as controllable PL (i.e., PL_1^c). As for the PV, the storage battery is used as an emulator instead of a real PV generator, which is responsible for supplying power based on user-defined values for each second. These user-defined values resemble dynamics of the real PV system. Additionally, we used a smart TV embedded with a processing unit and memory for advanced functionalities.

In this experiment, the roles of master and slave to power devices, PFP, and PFS are assigned manually. That is, there are

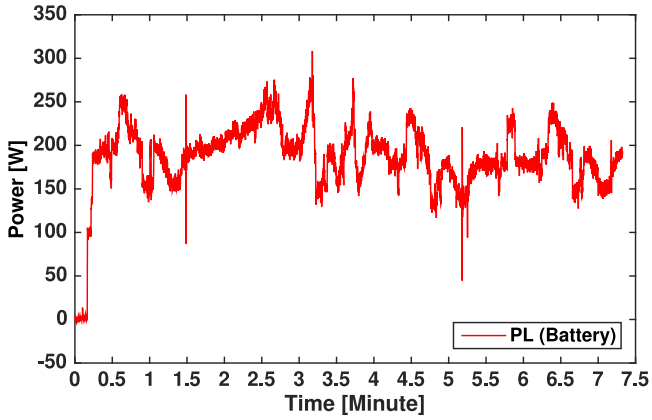

Fig. 11. Power consumption of battery PL.

no EoD manager and PFM in this experimental setup. The PFP and power ratio computations (both global and local ratios) in the PFS are given as

$$\mathrm{PFP} = \begin{array}{c} \\ \mathrm{PS}_1^c \\ \mathrm{PS}_2^c \\ \mathrm{PS}_1^f \end{array} \begin{array}{c} \begin{array}{ccc} \mathrm{PL}_1^c & \mathrm{PL}_1^f & \mathrm{PL}_2^f \end{array} \\ \begin{bmatrix} 50W & 20W & 45W \\ 50W & 15W & 45W \\ 50W & 15W & 90W \end{bmatrix} \end{array}$$

$$\mathrm{PFS} = \begin{array}{c} \\ \mathrm{PS}_1^c \\ \mathrm{PS}_2^c \\ \mathrm{PS}_1^f \\ \\ \mathrm{PCR} \end{array} \begin{array}{c} \begin{array}{ccc} \mathrm{PL}_1^c & \mathrm{PL}_1^f & \mathrm{PL}_2^f \end{array} \\ \left[\begin{array}{c|cc} 50W & 20/35 & 45/90 \\ 50W & 15/35 & 45/90 \\ \hline 50/50 & (15/50) & (90/180) \\ & (15/155) & (90/155) \end{array}\right] \end{array} \begin{array}{c} \\ \\ \mathrm{PSR} \\ \mathrm{GPSR} \\ \mathrm{GPCR} \end{array}$$

Here, PL_1^f is presented as a TV, and PL_2^f is a fan. The total time duration of the experiment is 7 min. The TS duration for feedback control is fixed to TS= 1 s.

The starting time or IP when time $t = 0$ (marked in graphs), all devices are switched OFF. During the IP, all power agents are well synchronized based on the ac cycle of 60 Hz. Then, the OP started (marked in graphs), in which all PSs (Figs. 8, 9, and 10) and PLs (Figs. 11, 12, and 13) start supplying and consuming power according to the PFS. Note that fluctuating PLs, i.e., TV and fan, are intentionally switched OFF in the beginning of the experiment to observe the power flow streams between controllable power devices.

According to the PFS, PS_1^c and PS_2^c should supply 50 W to PL_1^c. Fig. 10 shows that the slave PS is supplying the specified power to PL_1^c, where master PS supplied 50 W to the same PL and also absorbed power fluctuations by PV. As described in the previous section, power control is conducted for controllable power devices after two TSs; the power supply by PV is absorbed by the master PS for the first two TSs of the OP. From TS_3, PL_1^c absorbed power supply by PV rather than master.

At time, $t = 1.5$, TV is initially connected to ac voltage (see Fig. 13). It took a brief moment for inductors and capacitors to get charged to where they react steadily with the alternating current. The power consumption of TV experienced sharp peak

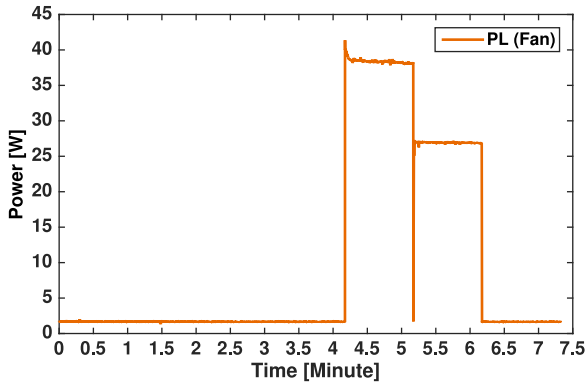

Fig. 12. Power consumption of the fan.

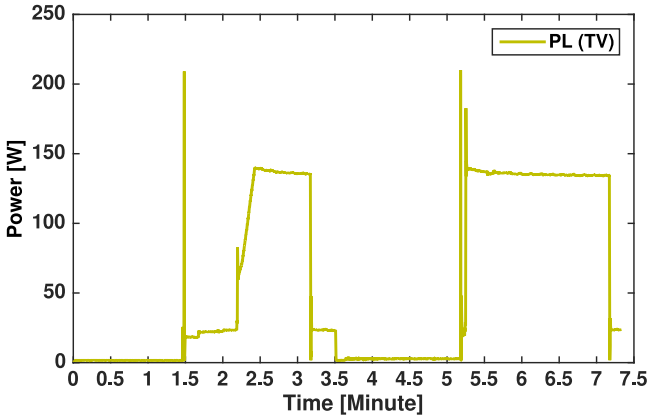

Fig. 13. Power consumption of TV.

due to inrush current, which, however, rapidly died down. After this warm-up period, the TV is switched ON manually for 1 min. At switched OFF time, power consumption of the standby mode is observed. All three PSs supplied ratio-based power to TV according to the PFS. Since the power consumption by TV changes largely, the power supply by PSs oscillate accordingly. Then, master SA_1^c automatically stabilizes (absorbs) the oscillation by maintaining the voltage level of the NG. Hence, no oscillation is observed in the power consumption TV, as shown in Fig. 13. After that, fan is switched ON manually and remained ON for 1 min with strong operating mode (see Fig. 12). The operating mode of the fan is shifted to the weak mode for one more minute and TV is switched ON at the same time (see Fig. 13). The TV remained switched ON for 2 min. This shows that all power devices are operating, which shows power flow streams.

In order to show the correctness of our proposed algorithm in managing power flow streams between fluctuating power devices, two quantitative analysis are presented in Figs. 14 and 15. We choose two extreme points (marked as TS_a and TS_b in Fig. 9), which show high and low PV generation. In Fig. 14 (high PV generation is discussed), power levels are assigned to fluctuating power devices according to the GPSR and the GPCR (calculated in black in Fig. 14). Note that the measured power levels for fluctuating devices are taken two TSs before from the recorded data of the experiment, i.e., MP_{a-2}. We got these power levels from log file created during the experiment.

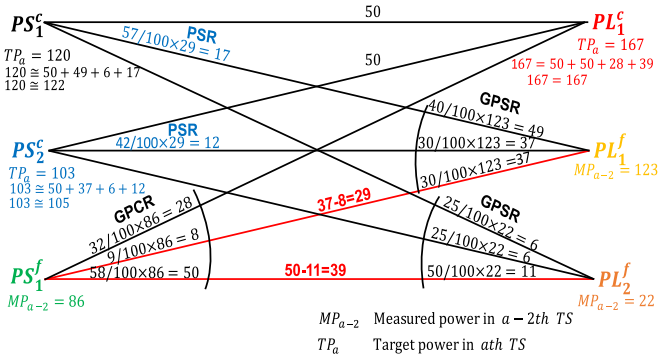

Fig. 14. Power fluctuation management with low PV power.

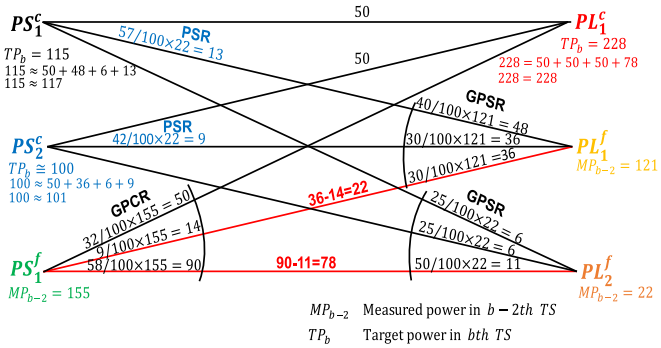

Fig. 15. Power fluctuation management with high PV power.

At first, the power flow stream between PS_1^f and PL_1^f would be solved. The conflict of assigned power levels for this particular power flow is solved by taking the difference (calculated in red). The difference of power levels is higher at the PL_1^f side. So, this difference is distributed among attached controllable power devices, i.e., PS_1^c and PS_2^c, based on local power ratios (computed in blue) in Fig. 14. Also, the difference of power levels for power flow between PS_1^f and PL_2^f is compensated by PL_1^c, as this is the only attached controllable device. The compensation is added to the new target power level for controllable power devices as TP_a (computed for all controllable devices in Fig. 14). This computation shows that the target power in the current TS based on measured data of two TSs before is nearly the same. This analysis also proves that the power supply to a specific load from multiple sources can be realized stably, i.e., no power oscillations are observed in power consumption of TV and fan (see Figs. 12 and 13), and local power ratios are preserved as shown in calculations for controllable power devices. From these calculations, we can see that the specified PSR and PCR are maintained accurately against large power variations of fluctuating PS.

Finally, we measured fluctuations of effective voltage at shared power bus to show the effectiveness of voltage stability control by the master SA working as a voltage source (see Fig. 16). We obtained the following statistical measures: number of measured samples: 4 395 582, average: 99.974 V, min: 97.412 V, max: 101.1000 V, and standard deviation: 0.1313 V. These measures verified that the voltage of power bus line is maintained stably.

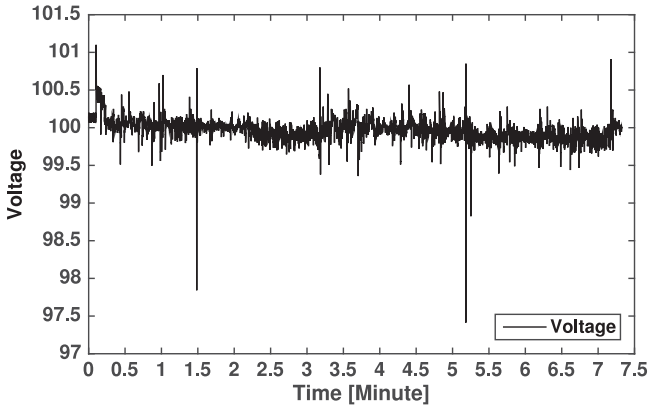

Fig. 16. Voltage stability.

VII. Concluding Remarks

In this paper, a cooperative distributed control method is proposed to implement the power flow coloring system over an NG with fluctuating PSs and loads, while keeping the voltage of the NG stable. The experimental results demonstrated that the proposed method can maintain voltage stability, keep the specified power ratios against power fluctuations, and accommodate communication and computation delays. For the implementation in real environment, the proposed system should be modified in the following ways:

1) an inter-OP for power compensation is required for long-run operation including change in the PFP;
2) how to change the role of master and slave during system operation;
3) how to manage reactive power;
4) how to handle noise and ambiguous data;
5) system ability to handle fail-safe problems.

References

[1] E. Harrison, D. Saad, and K. Y. M. Wong, "Message passing for distributed optimisation of power allocation with renewable resources," in *Proc. 2nd Int. Conf. Intell. Green Build. Smart Grid*, 2016, pp. 1–6.
[2] D. Brown and C. Koravos, Japan's FIT: Flying too close to the sun?, 2014. [Online]. Available: https://www.dlapiper.com/media/Files/Insights/Publications/2014/10/Japans-fit
[3] N. Y. Dahlan, M. A. Jusoh, and W. N. A. W. Abdullah, "Solar grid parity for Malaysia: Analysis using experience curves," in *Proc. IEEE 8th Power Eng. Optim. Conf.*, 2014, pp. 641–466.
[4] E. Eusebio and C. Camus, "Residential PV systems with battery backup power attained already grid parity?," in *Proc. 13th Int. Conf. Eur. Energy Market*, 2016, pp. 1–5.
[5] M. H. Shwehdi and S. R. Muhammad, "Proposed smart DC nano-grid for green buildings a reflective view," in *Proc. Int. Conf. Renew. Energy Res. Appl.*, 2014, pp. 765–769.
[6] M. C. Kinn, "Proposed components for the design of a smart nano-grid for a domestic electrical system that operates at below 50 V DC," in *Proc. IEEE PES Int. Conf. Exhib. Innovative Smart Grid Technol.*, 2011, pp. 1–7.
[7] W. Zhang, F. C. Lee, and P. Y. Huang, "Energy management system control and experiment for future home," in *Proc. IEEE Energy Convers. Congr. Expo.*, 2014, pp. 3317–3324.
[8] N. Hatziargyriou, H. Asano, R. Iravani, and C. Marnay, "Microgrids," *IEEE Power Energy Mag.*, vol. 5, no. 4, pp. 78–94, Jul./Aug. 2007.
[9] T. Matsuyama, "Creating safe, secure, and environment-friendly lifestyles through i-Energy," *New Breeze*, vol. 21, no. 2, pp. 1–8, 2009.
[10] T. Matsuyama: "i-Energy: Smart demand-side energy management," in *Smart Grid Application and Development*. New York, NY, USA: Springer, 2014, ch. 8.
[11] S. Javaid, Y. Kurose, T. Kato, and T. Matsuyama, "Cooperative distributed control implementation of the power flow coloring over a nano-grid with fluctuating power loads," *IEEE Trans. Smart Grid*, vol. 8, no. 1, pp. 342–352, Jan. 2017.
[12] D. Forfia, M. Knight, and R. Melton, "The view from the top of the mountain: Building a community of practice with the gridwise trasactive energy framework," *IEEE Power Energy Mag.*, vol. 14, no. 3, pp. 25–33, May/Jun. 2016.
[13] K. Kok and S. Widergren, "A society of devices: Integrating intelligent distributed resources with transactive energy," *IEEE Power Energy Mag.*, vol. 14, no. 3, pp. 34–45, May/Jun. 2016.
[14] Y. Okabe and K. Sakai, "QoEn (quality of energy) routing toward energy on demand service in the future internet," Inst. Electr., Inf. Commun. Eng., Tech. Rep. IA2009-47(2009-10), 2009.
[15] T. Takuno, Y. Kitamori, R. Takahashi, and T. Hikihara, "AC power routing system in home based on demand and supply utilising distributed power sources," *Energies*, vol. 4, pp. 717–726, 2011.
[16] R. Abe, H. Taoka, and D. McQuilkin, "Digital Grid: Communicative electrical grids of the future," *IEEE Trans. Smart Grid*, vol. 2, no. 2, Jun. 2011.
[17] R. Takahashi, K. Tashiro, and T. Hikihara, "Router for power packet distribution network: Design and experimental verification," *IEEE Trans. Smart Grid*, vol. 6, no. 2, pp. 618–626, Mar. 2015.
[18] T. Kato, K. Yuasa, and T. Matsuyama, "Energy on demand: Efficient and versatile energy control system for home energy management," *Proc. SmartGridComm*, 2011, pp. 410–415.
[19] T. Kato, K. Tamura, and T. Matsuyama, "Adaptive storage battery management based on the energy on demand protocol," in *Proc. IEEE 3rd Int. Conf. Smart Grid Commun.*, 2012, pp. 43–48.
[20] T. Edagawa, K. Fukae, and T. Hisakado, "Peer-to peer energy transmission system by bidirectional AC-DC converter module," (in Japanese), Inst. Elect. Eng. Japan, Tech. Rep. PE-14-191, 2014.

Saher Javaid received the Bachelor's degree in computer science and the Master's degree in information technology from Allama Iqbal Open University, Islamabad, Pakistan, in 2004 and the University of the Punjab, Lahore, Pakistan, in 2007, respectively. She received the Ph.D. degree in information science from Japan Advanced Institute of Science and Technology, in 2014.

Since 2014, she has been working as an Assistant Professor in Kyoto University, Kyoto, Japan. Her research interests include distributed sensing and control and smart energy management systems.

Takekazu Kato (M'03) received the B.S. and D.S. degrees from Okayama University, Okayama, Japan, in 1997 and 2001, respectively.

He is currently an Associate Professor in the Graduate School of Informatics, Kyoto University, Kyoto, Japan. His research interests include pattern recognition, computer vision, and energy management. He is a member of the IEEE Communications Society, IPSJ, and IEICE.

Takashi Matsuyama received the B.Eng., M.Eng., and D.Eng. degrees in electrical engineering from Kyoto University, Kyoto, Japan, in 1974, 1976, and 1980, respectively.

He is currently a Professor in the Department of Intelligence Science and Technology, Graduate School of Informatics, Kyoto University. He studied cooperative distribute sensing-control-reasoning systems for more than 30 years. Their application fields include knowledge-based image understanding, visual surveillance, 3-D video, human–computer interaction, and smart energy management. He has written more than 100 journal papers and more than 20 books including three research monographs.